Materials Science and Engineering B 177 (2012) 744–749

Contents lists available at SciVerse ScienceDirect

Materials Science and Engineering B

journal homepage: www.elsevier.com/locate/mseb

Short communication

Chemical substitution of Cd ions by Hg in CdSe nanorods and nanodots: Spectroscopic and structural examination

Anatol Prudnikau[a], Mikhail Artemyev[a,d,*], Michael Molinari[b], Michel Troyon[b], Alyona Sukhanova[b,d], Igor Nabiev[b,d], Alexandr V. Baranov[c], Sergey A. Cherevkov[c], Anatoly V. Fedorov[c]

[a] Institute for Physico-Chemical Problems, Belarussian State University, 220030 Minsk, Belarus
[b] Université de Reims Champagne-Ardenne, 51100 Reims, France
[c] Saint-Petersburg State University of Information Technologies, Mechanics and Optics, St.-Petersburg 197101, Russia
[d] Laboratory of Nano-Bioengineering, Moscow Engineering Physics Institute, 31 Kashirskoe sh., 115409 Moscow, Russian Federation

ARTICLE INFO

Article history:
Received 12 July 2011
Received in revised form
15 December 2011
Accepted 23 December 2011
Available online 9 January 2012

Keywords:
CdSe
HgSe
Quantum dots
Nanorods
Chemical substitution
Spectroscopy

ABSTRACT

The chemical substitution of cadmium by mercury in colloidal CdSe quantum dots (QDs) and nanorods has been examined by absorption, photoluminescence and Raman spectroscopy. The crystalline structure of original CdSe QDs used for Cd/Hg substitution (zinc blende versus wurtzite) shows a strong impact on the optical and structural properties of resultant $Cd_xHg_{1-x}Se$ nanocrystals. Substitution of Cd by Hg in isostructural zinc blende CdSe QDs converts them to ternary $Cd_xHg_{1-x}Se$ zinc blende nanocrystals with significant NIR emission. Whereas, the wurtzite CdSe QDs transformed first to ternary nanocrystals with almost no emission followed by slow structural reorganization to a NIR-emitting zinc blende $Cd_xHg_{1-x}Se$ QDs. CdSe nanorods with intrinsic wurtzite structure show unexpectedly intense NIR emission even at early Cd/Hg substitution stage with PL active zinc blende $Cd_xHg_{1-x}Se$ regions.

1. Introduction

Besides controlling the size and shape of semiconductor quantum dots (QDs) the variation in the chemical composition is another way to control their optical properties. Highly luminescent ternary nanocrystals like $Zn_xCd_{1-x}Se$, $CdSe_xTe_{1-x}$, $Zn_xCd_{1-x}S$, etc. may cover the spectral range of emission not easily achievable by their binary analogs [1–3]. Ternary cadmium-mercury chalcogenides are of especial interest, since they can emit the light in the near-IR region which is important for practical applications in biomedical diagnostics and optoelectronics [4]. Earlier, mercury-containing ternary QDs have been synthesized either by direct reaction between Cd or Zn and Hg ions and chalcogen precursors (H_2S, NaHSe, NaHTe, etc.) in aqueous solutions or chemical substitution of Cd by Hg in preformed cadmium chalcogenide nanocrystals [4–8]. The synthesis of Hg-containing ternary QDs in organic solutions would be favorable for certain practical applications when the luminescent QDs must be introduced into hydrophobic polymeric films, beads, etc. It is of especial interest to use the cationic substitution reaction instead of direct QD synthesis from the mixture of Cd and Hg precursors, since one may start from cadmium chalcogenide nanocrystals of well controlled size and shape and try to preserve these parameters during Cd/Hg substitution. For example, Cd by Hg substitution in CdSe nanorods could result in nanoheterogeneous structures, similar to CdS or CdSe nanorods with Cd partially substituted by Ag, Pd or Pt [9,10]. Such semiconductor nanoheterostructures will be interesting objects for studying the collective effects in the ensemble of interacting quantum dots. From the other hand, Cd by Hg chemical substitution in CdSe nanorods may result in the formation of NIR-emitting ternary nanorods. The semiconductor nanorods exhibit unique optical properties. Unlike spherical quantum dots, the nanorods selectively absorb and emit linearly polarized light [11,12]. This is very important property which allows for the formation of polarization-sensitive micro-and nanoemitters or photodetectors [12,13]. Highly luminescent semiconductor nanorods can be used as a novel type of fluorescent tags for biomedical applications [14]. NIR region is of especial interest for utilization of fluorescent tags, since, the NIR emission is weakly absorbed by tissue, as compared to the visible light. Only few examples of NIR emitting one-dimensional nanowires or nanorods

* Corresponding author. Tel.: +375 172 891078; fax: +375 172 264696.
E-mail address: m_artemyev@yahoo.com (M. Artemyev).

0921-5107/$ – see front matter © 2011 Elsevier B.V. All rights reserved.
doi:10.1016/j.mseb.2011.12.038

were demonstrated earlier, including CdTe and PbSe nanowires and nanorods [15–18]. Here, we demonstrate, that the ternary CdHgSe nanorods emitting in the NIR region can be prepared by cationic substitution in CdSe nanorods.

Another interesting point is the cationic substitution in the nanocrystals of the same shape (e.g. QDs) with different crystalline structure. HgSe has only a cubic (zinc blende, ZB) stable phase at normal conditions, while CdSe QDs can be easily synthesized either with ZB, or hexagonal (Wurtzite, WZ) structure [19,20]. Here, we report on the spectroscopic and structural examination of Cd/Hg chemical substitution in CdSe quantum dots of ZB or WZ crystalline structure and CdSe nanorods (always WZ) in toluene colloidal solutions at mild conditions (30 °C). We demonstrate that the crystalline structure of original CdSe nanocrystals plays a crucial role in the luminescent properties of $Cd_xHg_{1-x}Se$ ternary nanocrystals obtained by Cd/Hg substitution.

2. Experimental part

ZB CdSe QDs of ca. 3.5 nm in diameter were synthesized according to published procedure by high temperature reaction between organometallic precursors in organic solutions [19]. WZ CdSe QDs of similar size were synthesized according to [20] and CdSe nanorods (NRs) of 3.5 nm in diameter and ca. 18 nm in the length according to [21]. The shape and the size of all nanocrystals were characterized by transmittance electron microscopy. After the synthesis the nanocrystals were purified by twofold deposition with methanol from their colloidal solutions in toluene or chloroform followed by dissolution in toluene with 30 vol.% of oleylamine (Aldrich) added to increase the solubility, colloidal stability and the luminescence quantum yield of nanocrystals. In preliminary experiments we failed to obtain stable colloidal solutions of ZB CdSe QDs in pure toluene without oleylamine. Mercury (II) benzoate (Aldrich) was dissolved in a minimum amount of tetraethylene glycol dimethyl ether (Aldrich) and added to the colloidal solution of QDs or NRs in toluene/oleylamine at 30 °C (the overall dilution rate has been kept less than 5 vol.%). The solution was stirred in sealed flask at 30 °C for up to 24 h and small aliquotes have been withdrawn and analyzed with optical absorption (Ocean Optics HR-2000) and fluorescence (Jobin-Yvon Fluoromax-2) spectrometers. For XRD analysis of crystalline structure of initial and substituted QDs and NRs the nanocrystals were deposited by adding 2-propanol, washed several times with methanol and dried to a powder. The elemental composition has been analyzed by EDX spectroscopy within the Leo 604 scanning electron microscopy. The Raman spectra of the samples were obtained in the backscattering geometry using an "inVia Renishaw" micro-Raman spectrometer with 50× objective and a CCD-detector cooled to −70 °C. A linearly polarized radiation of 514.5 nm of Ar+ laser was used for the Raman excitation. The laser power has been chosen as weak as ~0.5 mW to avoid irreversible thermal degradation of the samples. Total accumulation time of a single spectrum was about 15 min. Samples of nanocrystals for the Raman measurements were prepared by depositing and drying a droplet of colloid dispersion of nanocrystals onto copper substrate. All optical measurements were done at room temperature.

3. Results and discussion

We started with the ZB CdSe QDs which were isostructural to ZB HgSe. The homogeneous chemical substitution of Cd by Hg in spherical QDs should produce the discontinuous raw of ternary nanocrystals with increased Hg/Cd ration depending on the reaction time and the initial concentration of mercury salt in the colloidal solution. We examined three concentrations, namely 10, 50 and 100 mol.% of Hg (II) ions relative to the total molar concentration of Cd atoms in all nanocrystals in the reaction mixture. To estimate the total amount of Cd atoms we determined first the amount of CdSe QDs in the reaction mixture by widely accepted optical method [22]. The total amount of Cd atoms has been derived from the optical data and the calculated molar weight of QDs. We do not expect sufficient variations in the molar absorption coefficient for ZB versus WZ CdSe QDs. The situation with molar absorption coefficient for CdSe NRs is more complicated due to anisotropic

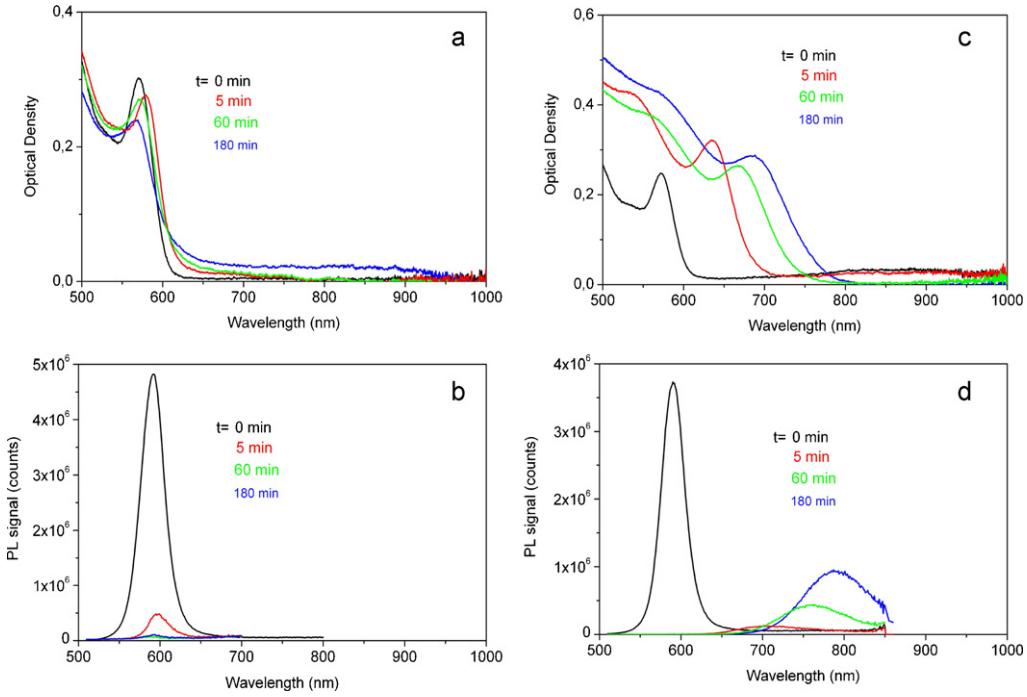

Fig. 1. Absorption (a and c) and photoluminescence (b and d) spectra of ZB CdSe quantum dots after their chemical treatment with 10 (a and b) or 100 mol.% (c and d) of mercury benzoate in toluene colloidal solution at 30 °C. The reaction time t is indicated on corresponding graphics. $\lambda_{ex}^{PL} = 500$ nm.

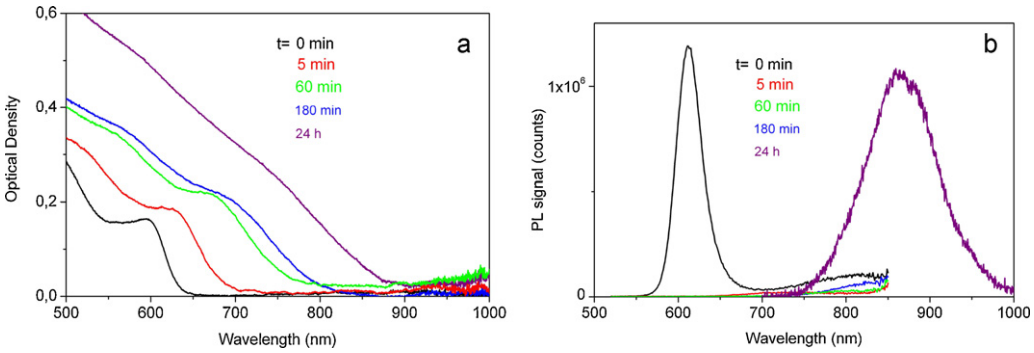

Fig. 2. Absorption (a) and photoluminescence (b) spectra of WZ CdSe quantum dots after their chemical treatment with 100 mol.% of mercury benzoate in toluene colloidal solution at 30 °C. The reaction time t is indicated on corresponding graphics. $\lambda_{ex}^{PL} = 500$ nm.

light absorption by NRs and one-dimensional nanowires, as well. The molar absorption coefficient for NRs has been estimated from the reference data for QDs of the same diameter multiplied by factor of V_{NR}/V_{QD}, where V_{NR} and V_{QD} were the molar volumes of NRs and QDs respectively, calculated from the geometrical size of nanocrystals determined by TEM [23].

Fig. 1 shows both absorption and photoluminescence (PL) spectra of ZB CdSe QDs treated with 10 and 100 mol.% of mercury benzoate. The reaction with 10 mol.% of mercury benzoate produces weak red shift of the first excitonic maximum in absorption spectra after the first 5 min of reaction. The absorption peak returns back to the initial position after ca. 60 min and accompanied with the increased absorption at the red tail. We attribute this effect to the formation of Hg-rich shell on the surface of ZB CdSe QDs in the first minutes of reaction followed by diffusion of Hg atoms inside QDs and homogenization of crystalline phase. Such small number of Hg atoms introduced into the CdSe phase was not enough to notably affect the band gap energy of CdSe QDs. In PL spectra we see almost complete quenching of QDs emission. This effect also can be explained by the formation of Hg-rich shell on the surface of CdSe QDs. Since, bulk HgSe is "zero"-gap semiconductor the excitonic recombination takes place in the low-band gap Hg-rich shell and exhibits mostly nonradiative character due to high defectness. The increase of mercury benzoate concentration results in the strong red shift and spectral broadening of excitonic absorption band due to formation of low-band gap $Cd_xHg_{1-x}Se$ phase. In the corresponding PL spectra we observed the formation and growth of NIR PL band which intensity reached ca. 25% of PL signal from original non-treated CdSe QDs. The Stokes shift between absorption and PL maxima increased with the reaction time and reached 0.2 eV for QDs treated with 100 mol.% of mercury benzoate at 180 min. The magnitude of Stokes shift is 3 times larger than for non-treated ZB CdSe QDs. Such large Stokes shift points to either a trap-like character of radiative recombination or the formation of ternary $Cd_xHg_{1-x}Se$ with Cd-rich core and Hg-rich shell. Similar, gradient $CdSe_xTe_{1-x}$ QDs have been synthesized earlier under Cd-rich conditions [2]. The relatively high PL intensity growing with the reaction time may be explained by the improved crystallinity of $Cd_xHg_{1-x}Se$ QDs and decreased amount of nonradiative recombination traps.

The chemical substitution in WZ CdSe QDs shows different spectral behavior as compared to ZB QDs, especially for high concentration of mercury benzoate. Chemical substitution with 10 mol.% of

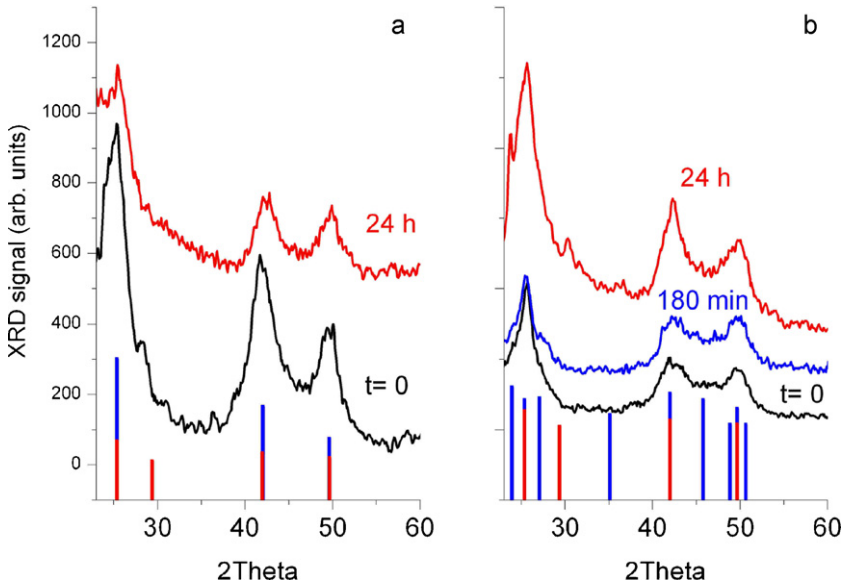

Fig. 3. XRD spectra (Cu $K\alpha_1$) of original (black) and substituted (blue and red) ZB (a) and WZ (b) CdSe quantum dots treated with 100 mol.% of mercury benzoate at 30 °C for different reaction times (blue – 180 min, red – 24 h). Blue and red bars at the bottom of part (a) indicate the position and relative intensities of the major XRD peaks for bulk ZB CdSe (blue bars, JCPDF Card No. 19-191) and ZB HgSe (red bars, JCPDS Card No. 8-469). Blue and red bars at the bottom of part (b) indicate the position and relative intensities of the major XRD peaks for bulk WZ CdSe (blue bars, JCPDS Card No. 8-459) and ZB HgSe (red bars). (For interpretation of the references to color in this figure legend, the reader is referred to the web version of this article.)

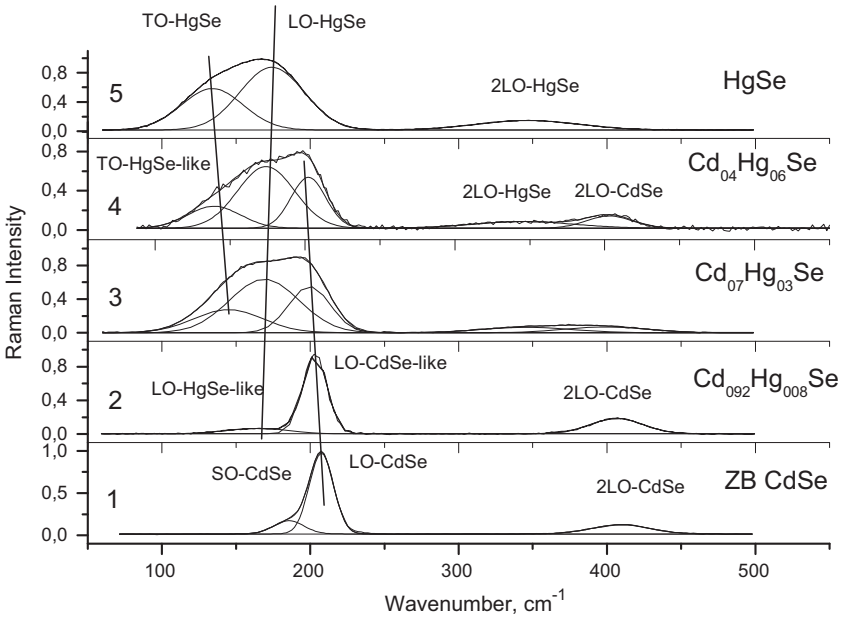

Fig. 4. Raman spectra of ZB quantum dots: CdSe (1), HgSe (5), and $Cd_xHg_{1-x}Se$ (2–4), where Hg content is 0.08, 0.3 and 0.6, respectively. Decomposition of Raman spectra with gaussian and assignment of the Raman bands to the optical phonon modes of materials are shown. The vertical lines are guides for eyes showing the shift of the bands position with increase of Hg content in CdHgSe quantum dots.

mercury benzoate produces only a small spectral shift of excitonic absorption band and almost complete PL quenching. Fig. 2 shows absorption and PL spectra of WZ CdSe QDs during the chemical substitution with 100 mol.% of mercury benzoate. The magnitude of the red shift in absorption spectra is similar to ZB QDs, while the spectral broadening is much larger in WZ QDs pointing to the less homogeneous quantum confinement system even at very long reaction time. The PL band is quenched completely immediately after addition of mercury benzoate followed by a minor growth with the reaction time up to 180 min. We believe that it is due to highly defect crystalline structure of substituted $Cd_xHg_{1-x}Se$ QDs with dominant nonradiative recombination of excited excitons. Surprisingly, 24 h stirring of the reaction mixture results in the appearance of intense NIR PL band with the maximum around 860 nm and the spectral linewidth of about 160 meV. The magnitude of the Stokes shift cannot be determined precisely due to large spectral broadening of corresponding excitonic absorption band. It is around 0.2 eV, close to the value obtained for substituted ZB QDs. In order to establish the correlation between the spectral behavior and the changes in the crystalline structure of substituted nanocrystals we did XRD analysis of ZB and WZ CdSe QDs before and after prolonged treatment with 100 mol.% of mercury benzoate (Fig. 3).

The chemical substitution of Cd by Hg in ZB CdSe phase expectedly produces ZB $Cd_xHg_{1-x}Se$ nanocrystals isostructural to bulk ZB HgSe. When the WZ CdSe phase undergoes the chemical treatment with 100 mol.% of mercury benzoate the exact determination of the type of crystalline phase and the lattice parameters for substituted WZ $Cd_xHg_{1-x}Se$ nanocrystals is hampered by very close lattice parameters for ZB CdSe and HgSe and strong size-broadening of XRD peaks. However, for $t = 0$ we see a weak peak at $2\theta = 45.8^\circ$ which belongs to CdSe WZ (1 0 3) plane (Fig. 3b). It is absent in ZB CdSe phase. Two neighboring peaks at $2\theta = 41.9^\circ$ and 49.6° correspond to (1 1 0) and (1 1 2) planes for WZ and ZB CdSe. 180 min chemical substitution does not affect strongly the relative intensities of (1 0 3), (1 1 0) and (1 1 2) peaks. Since, WZ crystalline structure is unknown for bulk HgSe the 180 min substitution in WZ CdSe QDs produces rather highly defect phase which can be derived from almost complete PL quenching of QDs shown in Fig. 2. Prolonged 24 h substitution results in a boost of (1 1 0) and (1 1 2) peaks and vanishing of (1 0 3) peak. We may attribute this effect to a conversion of intermediate WZ-like $Cd_xHg_{1-x}Se$ phase to ZB phase. Therefore, the appearance of intense NIR PL band after 24 h substitution in WZ CdSe QDs can be assigned to the formation of less defect ZB $Cd_xHg_{1-x}Se$ QDs similar to the case of Cd/Hg substitution in ZB-phase CdSe QDs. Such a long substitution time (24 h) required to complete the conversion of WZ CdSe to ZB $Cd_xHg_{1-x}Se$ may be explained by relatively low (30 °C) reaction temperature. We tried to conduct the same process at much higher temperature (90 °C in toluene), but faced with the problem of limited stability of colloidal solutions of substituted QDs at higher temperature (aggregation). The chemical composition of substituted $Cd_xHg_{1-x}Se$ QDs determined by EDX points to the $Cd_{0.4}Hg_{0.6}Se$ structure when obtained from ZB CdSe QDs and $Cd_{0.65}Hg_{0.35}Se$ from WZ QDs. Almost twice less amount of mercury introduced in the WZ CdSe QDs during chemical substitution as compared to ZB QDs may be an additional indication of hampered substitution process in non-isostructural system.

The precise XRD examination of the changes in the crystalline phase of CdSe QDs during Cd/Hg chemical substitution is limited

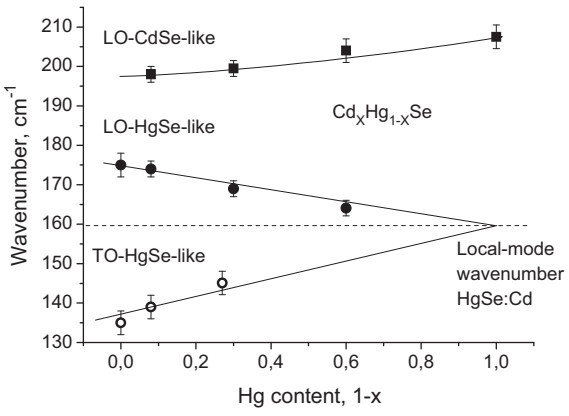

Fig. 5. Wavenumbers of phonon modes in Raman spectra of ZB $Cd_xHg_{1-x}Se$ quantum dots as a function of Hg content, $1 - x$. The local-mode wavenumber of ~160 cm^{-1} is shown. The lines are guides for eyes.

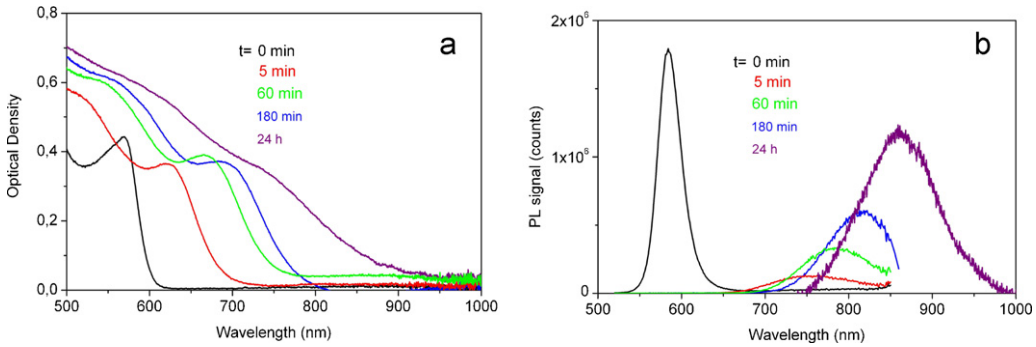

Fig. 6. Absorption (a) and photoluminescence (b) spectra of WZ CdSe nanorods after their chemical treatment with 100 mol.% of Hg benzoate in toluene colloidal solution at 30 °C. The reaction time t is indicated on corresponding graphics. $\lambda_{ex}^{PL} = 500$ nm.

by strong broadening of XRD peaks and close lattice parameters for ZB and WZ CdSe and for ZB HgSe. Here, we additionally use Raman spectroscopy analysis of substituted ZB $Cd_xHg_{1-x}Se$ QDs, since the Raman bands for ZB CdSe and HgSe are well separated. Earlier, the Raman spectroscopy has been proved to be a sensitive tool for examination of thin semiconductor shell atop the core in CdSe/ZnS core–shell QDs [24]. A representative set of Raman spectra of ZB CdSe QDs treated with 10, 50, and 100 mol.% of mercury benzoate during 24 h is shown in Fig. 4. The Raman spectra of original ZB CdSe QDs and ZB HgSe are also shown for comparison. The spectrum of original ZB CdSe QDs demonstrates the well-known Raman bands of surface (SO) and longitudinal (LO) optical phonons, and 2LO overtone at 186 cm^{-1}, 207.5 cm^{-1} and 409 cm^{-1}, respectively [24]. The TO-phonon band of CdSe QDs was not observable because of the resonant nature of Raman excitation. The Raman spectrum of HgSe QDs shows the bands of TO, LO and 2LO phonons at 135 cm^{-1}, 175 cm^{-1} and 346 cm^{-1} which are in good agreement with the energies of corresponding phonons in a bulk HgSe at room temperature [25]. Both the LO and TO phonon bands are observed in Raman spectra of HgSe QDs since the incident photon energy is far from fundamental optical transition of the nanocrystals. The large width of the Raman bands (>40 cm^{-1}) probably indicates the presence of some lattice disorder in HgSe QDs.

Fig. 4 shows that the chemical substitution of cadmium with mercury atoms results in the appearance of new 1st and 2nd order Raman bands with the wavenumbers in the region expected for the TO, LO and 2LO bands of HgSe QDs. Importantly, position and relative intensity of these bands, as well as the LO and 2LO bands attributed to CdSe QDs depend on Hg content in the CdHgSe QDs. The position of bands in 1st order Raman spectra of $Cd_xHg_{1-x}Se$ QDs versus the Hg content is shown in Fig. 5. It clearly

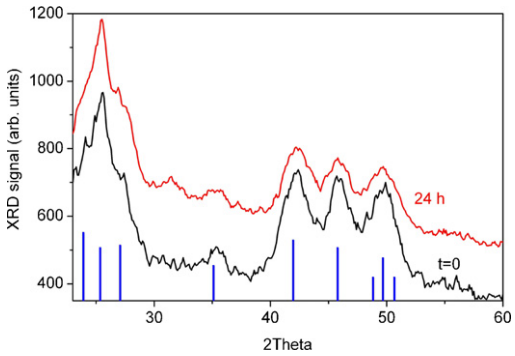

Fig. 7. XRD spectra (Cu $K\alpha_1$) of original WZ CdSe nanorods (black) and after 24 h treatment with 100 mol.% of mercury benzoate (red) at 30 °C. Blue bars demonstrate the position and relative intensities of the major XRD peaks for bulk WZ CdSe (JCPDS Card No. 8-459). (For interpretation of the references to color in this figure legend, the reader is referred to the web version of this article.)

demonstrates the classic two-mode behavior of lattice vibrations in CdSe QDs treated with 10, 50, and 100 mol.% of mercury benzoate and therefore indicates the formation of $Cd_xHg_{x-1}Se$ ternary compound.

Finally, we examined the chemical Cd/Hg substitution in CdSe NRs with intrinsic WZ crystalline structure. CdSe NRs are formed by unidirectional chemical growth along WZ c-axis in the presence of alkylphosphonic acids [22]. Apriori, we would expect a similar spectral behavior for CdSe NRs, as for WZ CdSe QDs during the chemical substitution. However, the results are drastically different. Fig. 6 shows absorption and PL spectra of WZ CdSe NRs treated with 100 mol.% of mercury benzoate for different reaction times. Immediately after the addition of mercury benzoate the

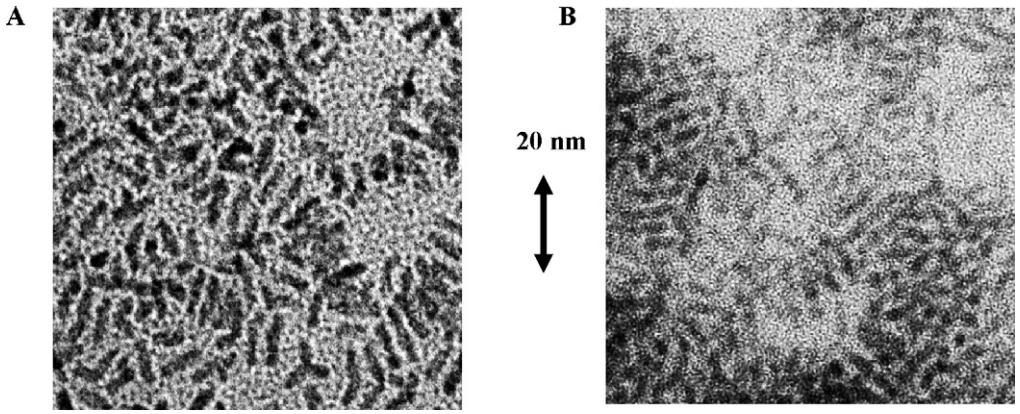

Fig. 8. TEM images of WZ CdSe nanorods before (a) and after (b) chemical treatment with 100 mol.% of Hg benzoate in toluene colloidal solution at 30 °C for 24 h.

CdSe excitonic PL band is quenched and a new band appeared at the red part of the spectrum. This new band is red shifted and grows in intensity with the reaction time. The parallel red shift and the spectral broadening of the excitonic bands are observed in the absorption spectra. The final (24 h) Stokes shift of PL band is around 0.21 eV, close to obtained earlier for substituted ZB and WZ QDs. Very recently, similar Cd/Hg substitution in CdSe NRs has been studied in [26], but the less pronounces changes in the absorption spectra observed together with almost complete PL quenching. We may explain these results by much shorter Cd/Hg substitution time in [26] as compared to our experiments.

The XRD spectra contain mostly the peaks from WZ CdSe or $Cd_xHg_{1-x}Se$ phase (Fig. 7). The WZ crystalline structure persists through the substitution process with apparent broadening of XRD peaks which may be caused by partial WZ-to-ZB phase transition. The elemental analysis of 24 h substituted WZ CdSe NRs points to the $Cd_{0.45}Hg_{0.55}Se$ chemical composition which is close to observed earlier for substituted ZB CdSe QDs. The one-dimensional rod-like morphology of CdSe NRs also remains practically unchanged which is seen from corresponding TEM images in Fig. 8(a and b). Now that a ZB CdHgSe phase is only a PL active we assume that Cd by Hg substitution in WZ CdSe NRs is going through the formation of nanoheterostructures with ZB Hg-rich regions (HgSe or $Cd_xHg_{1-x}Se$) in WZ CdSe nanorods. Significant room temperature NIR PL signal from substituted CdSe NRs may be explained by efficient radiative recombination through the narrow-gap ZB $Cd_xHg_{1-x}Se$ regions.

4. Conclusions

The chemical transformation of binary CdSe to ternary $Cd_xHg_{1-x}Se$ nanocrystals via Cd by Hg cationic substitution in toluene colloidal solution is strongly influenced by the morphology and crystalline phase of original CdSe nanocrystals. Zinc blende CdSe quantum dots can be easily converted to isostructural $Cd_xHg_{1-x}Se$ dots emitting in the NIR region whereas the wurtzite CdSe QDs require extended substitution time necessary to convert hexagonal CdSe crystalline phase to a zinc blende $Cd_xHg_{1-x}Se$. CdSe nanorods with intrinsic wurtzite structure show unusual optical behavior during cationic substitution, similar to zinc blende QDs which may point to the formation of nanoheterostructure with efficient radiative recombination in the narrow gap ZB $Cd_xHg_{1-x}Se$ regions.

Acknowledgments

This work was supported by the Belarussian CHEMREAGENTS program and NATO SfP-983-207 Grant. I.N. and A.S. acknowledges partial support from EU FP7-program through NMP-2009-4.0-3-246479 project NAMDIATREAM. M.A. acknowledges visiting Professor fellowship to University of Reims. We thank Prof. T. Niermann and his colleagues from the Technical University of Berlin for help with TEM. I.N., A.S., and M.A. acknowledge also the Ministry of Higher Education and Science of the Russian Federation (grant no. 11.G34.31.0050).

References

[1] X. Zhong, M. Han, Z. Dong, T.J. White, W. Knoll, J. Am. Chem. Soc. 123 (2003) 8589.
[2] R.E. Bailey, S. Nie, J. Am. Chem. Soc. 125 (2003) 7100.
[3] X. Zhong, Y. Feng, W. Knoll, M. Han, J. Am. Chem. Soc. 125 (2003) 13559.
[4] A.L. Rogach, A. Euchmüller, S.G. Hickey, S.V. Kershaw, Small 3 (2007) 536.
[5] F.-C. Liu, Y.-M. Chen, J.-H. Lin, W.-L. Tseng, J. Colloid Interface Sci. 337 (2009) 414.
[6] H. Quian, C. Dong, J. Peng, X. Qiu, Y. Xu, J. Ren, J. Phys. Chem. C 111 (2007) 16852.
[7] S. Taniguchi, M. Green, T. Lim, J. Am. Chem. Soc. 133 (2011) 3328–3331.
[8] A.M. Smith, S. Nie, J. Am. Chem. Soc. 133 (2011) 24–26.
[9] R.D. Robinson, B. Sadtler, D.O. Demchenko, C.K. Erdonmez, L.-W. Wang, A.P. Alivisatos, Science 317 (2007) 355.
[10] S.E. Wark, C.-H. Hsia, D.H. Son, J. Am. Chem. Soc. 130 (2008) 9550.
[11] J. Wang, M.S. Gudiksen, X. Duan, Y. Ciu, C.M. Lieber, Science 293 (2001) 1455.
[12] J. Hu, L.S. Li, W. Yang, L. Manna, L.W. Wang, A.P. Alivisatos, Science 292 (2001) 2060.
[13] M. Artemyev, B. Moller, U. Woggon, Nano Lett. 3 (2003) 509.
[14] A.H. Fu, W.W. Gu, B. Boussert, K. Koski, D. Gerion, L. Manna, M. Le Gros, C. Larabell, A.P. Alivisatos, Nano Lett. 7 (2007) 179.
[15] D.V. Talapin, H. Yu, E.V. Shevchenko, A. Lobo, C.B. Murray, J. Phys. Chem. C 111 (2007) 14049.
[16] D.V. Talapin, C.T. Black, C.R. Kagan, E.V. Shevchenko, A. Afzali, C.B. Murray, J. Phys. Chem. C 111 (2007) 13244.
[17] Z. Hu, M.D. Fischbein, C. Querner, M. Drndić, Nano Lett. 6 (2006) 2585.
[18] J. Sun, W.E. Buhro, L.W. Wang, J. Schrier, Nano Lett. 8 (2008) 2913.
[19] H. Shen, H. Wang, Z. Tang, J.Z. Niu, S. Lou, Z. Du, L.S. Li, Cryst. Eng. Commun. 11 (2009) 1733.
[20] Z. Peng, X. Peng, J. Am. Chem. Soc. 124 (2002) 3343.
[21] X. Peng, L. Manna, W. Yang, J. Wickham, E. Scher, A. Kadavanich, A.P. Alivisatos, Nature 404 (2000) 59.
[22] W.W. Yu, L. Qu, W. Guo, X. Peng, Chem. Mater. 15 (2003) 2854;
W.W. Yu, L. Qu, W. Guo, X. Peng, Chem. Mater. 16 (2004) 560.
[23] M. Artemyev, E. Ustinovich, I. Nabiev, J. Am. Chem. Soc. 131 (2009) 8061.
[24] A.V. Baranov, Yu.P. Rakovich, J.F. Donegan, T.S. Perova, R.A. Moore, D.V. Talapin, A.L. Rogach, Y. Masumoto, I. Nabiev, Phys. Rev. B 68 (2003) 165306.
[25] (a) K. Kumazaki, Phys. Status Solidi B 151 (1989) 353;
(b) K. Kumazaki, Phys. Status Solidi B 160 (1990) K173.
[26] S. Taniguchi, M. Green, J. Mater. Chem. 21 (2011) 11592.